Eur. Phys. J. Plus (2024) 139:1137
https://doi.org/10.1140/epjp/s13360-024-05914-5

THE EUROPEAN PHYSICAL JOURNAL PLUS

Regular Article

Effect of anisotropy, inhomogeneity and porosity on love wave propagation through fluid-saturated porous layers in irregular layered media

Ravinder Kumar[a], **Abhilasha Saini**[b]

Department of Mathematics, Chandigarh University, Mohali 140413, India

Received: 12 June 2024 / Accepted: 9 December 2024
© The Author(s), under exclusive licence to Società Italiana di Fisica and Springer-Verlag GmbH Germany, part of Springer Nature 2024

Abstract The present paper investigates the propagation of Love waves through a fluid-saturated porous layer sandwiched between isotropic homogeneous layer and non-homogeneous elastic half space with an irregular interface. A point source is considered at a particular depth in the half space causing a parabolic irregularity at the interface of the porous layer and half space. The study utilizes Biot's theory of elasticity and applies Fourier transformation to derive analytical solution. The computational simulations of dispersion equation using MATLAB reveal key outcomes: Phase velocity decreases with an increase in inhomogeneity, anisotropy, and porosity factors, a significant reduction in wave velocity is observed with increasing wave number, and irregularity depth to layer's height ratio affects wave propagation significantly, diminishing phase velocity. The study reveals several key quantitative outcomes as, phase velocity decreases by up to 15% as the inhomogeneity parameter increases from 0 to 3, anisotropy causes a reduction in phase velocity by 10–12%, and porosity results in a 20–25% decrease in wave velocity. Additionally, increasing the depth ratio of the irregularity leads to a 30% reduction in phase velocity. The findings of this study provide deeper insights into Love wave behavior across layered media, which have practical implications for geophysics, seismology, fluid mechanics and earthquake engineering.

List of symbols

Parameter	Description
ε	Small positive number
l	Depth of irregularity
2s	Width of irregularity
σ_{ij}, $i, j = 1, 2, 3$	Component of stress tensor in M_1
τ_{ij}, $i, j = 1, 2, 3$	Component of stress tensor in M_2
t_{ij}, $i, j = 1, 2, 3$	Component of stress tensor in M_3
u_i, $i = 1, 2, 3$	Displacement components of M_1
v_i, V_i, $i = 1, 2, 3$	Displacement components of fluid and solid skeleton of M_2
w_i, $i = 1, 2, 3$	Displacement components of M_3
H_1 and H_2	Height of layer 1 and 2
δ_{ij}, $i, j = 1, 2, 3$	Lame's constants for medium 1, 2 and 3
δ_{ij}, $i, j = 1, 2, 3$	Kronecker delta
$C_1, C_2, ..., C_8$	Elastic constants of M_2
f	Fluid porosity and pressure of M_2
ρ_{ij}, $i, j = 1, 2, 3$	Mass density coefficients of M_2
ω	Angular velocity
μ_0, ρ_0	Arbitrary constants

[a] e-mail: ravinderpoonia25@gmail.com (corresponding author)
[b] e-mail: abhilashasaini21@gmail.com

Published online: 31 December 2024

1 Introduction

The study of Love waves is crucial in fields like seismology, geophysics, and engineering due to their significant impact on surface phenomena. In earthquake engineering, Love waves are particularly important as they cause extensive horizontal ground displacements, often leading to major damage during seismic events. Understanding Love waves can help scientists predict and limit the effects of ground motion, contributing to the development of earthquake-resistant designs. The Earth contains fluid-saturated porous layers, such as sandstone and sedimentary formations infused with groundwater or oil. The behavior of Love waves in these porous layers has gained considerable attention due to its relevance in soil mechanics, ocean engineering, and earthquake engineering. These layers can be anisotropic, isotropic, or transversely isotropic in nature. Additionally, the movement and redistribution of fluids, along with changes in fluid pressure, can act as triggers for earthquakes. Valuable insights into the propagation of seismic waves in fluid-saturated porous mediums can be found in the books Ewing et al. [1] and Gubbins [2]. Biot [3, 4] developed the theory of propagation of elastic waves in a fluid-saturated porous material and formulated the equation of motion for elastic waves in two-phase systems (fluid phase and solid phase). This study predicted the presence of two types of dilatational waves and one shear wave propagating through a porous medium. Deresiewicz [5] was the first to derive the dispersion equation for Love waves in a porous solid. However, this work did not provide dispersion and attenuation curves for Love waves. Since then, many researchers have applied Biot's theory to a variety of problems involving the propagation of seismic waves through the Earth's porous layers. Chattopadhyay and De [6] examined Love wave propagation in a fluid-saturated isotropic porous layer over a non-homogeneous half-space characterized with a rectangular irregularity at the interface of the layer and half-space. Dutta and Odé [7] gave a theory for attenuation and dispersion of seismic waves in fluid-saturated porous rocks with partial gas saturation. Wang and Zhang [8] extended this research by investigated Love wave propagation in a layer over a half-space; both layer and half-space are taken to be transversely isotropic fluid-saturated porous solids. Their study employed an effective iterative method to resolve the complex dispersion equation, providing analytical representations of the upper and lower bounds of Love wave speed in such media. Crampin [9] examined the propagation of the surface wave in a fluid-saturated medium. This study emphasized the significant role of the fluid within the pores of a medium for the occurrence and preparation of the earthquake. Konczak [10] studied propagation of Love waves in a fluid-saturated anisotropic porous layer overlaying an elastic, nonhomogeneous half space, graphically illustrating the effects of material heterogeneity and anisotropy on wave behavior. Additionally, Carcione and Seriani [11] applied a numerical algorithm to analyze wave propagation in frozen porous media, where pores are partially or completely filled with water and ice, demonstrating the distinctive effects of temperature and pore content on wave speed and attenuation. Sharma [12] analyzed surface wave propagation in a general anisotropic poroelastic solid half space. This research compared the characteristics of Love waves in three different types of top anisotropic porous media: monoclinic, triclinic, and orthorhombic. Chattopadhyay et al. [13] have studied the propagation of Love waves in a composite isotropic structure and examined the effect of inhomogeneity on the phase velocity of Love waves. Ke et al. [14, 15] analyzed Love wave propagation using an iterative method in a fluid-saturated porous layer resting over a half-space, where the porous layer is transversely isotropic with linearly varying properties. This study offered a refined approach to resolving complex dispersion relationships in such media. Kumar et al. [16, 17] investigated surface wave propagation in a layered medium featuring a transversely isotropic porous layer sandwiched between a homogeneous isotropic layer and a non-homogeneous elastic half-space. They considered various boundary conditions and the effect of a rectangular irregularity at the interface of the porous layer and half-space, adding further depth to the study of interface effects on wave propagation.

Kakar [18], Vaishnav et al. [19], and Gupta et al. [20] investigated Love wave propagation in porous layers with irregular or welded interfaces. Kakar focused on a layer over a nonhomogeneous half-space under initial stress, Vaishnav et al. examined a porous medium on an orthotropic semi-infinite medium, and Gupta et al. studied the effect of initial stress in an anisotropic porous layer in welded contact with a nonhomogeneous elastic half-space. Kundu et al. [21] analyzed the propagation of shear waves through a viscoelastic layer sandwiched between an anisotropic porous layer of finite thickness and an isotropic half space. Kumhar et al. [22] gave a study on the propagation of Love waves in an initially stressed anisotropic porous medium resting over an inhomogeneous isotropic half-space influenced by gravity. Kumar et al. [23] studied shear wave propagation in a fluid-saturated porous layer over heterogeneous elastic half-space with triangular shaped interface irregularity. Kumar and Saini [24] explored the influence of inhomogeneity, initial stress, anisotropy, and interface irregularity on the propagation of Love waves within a transversely isotropic porous layer over a nonhomogeneous elastic half space. This study uses Biot's theory of elasticity and perturbation technique to find the dispersion equation of the wave. This research graphically highlighted the influence of these parameters including the ratio of layer's depth and height of irregularity on the phase and velocity of the Love wave. Saini and Kumar [25, 26] investigated Love wave propagation in fluid-saturated porous media, focusing on the effects of rigidity, initial stress, and mainly parabolic-shaped irregularity at the interface of porous layer and elastic half space. Seikh et al. [27] studied the propagation of localized waves in a transversely isotropic thermoelastic layer of arbitrary thickness.

Previous studies in this field have primarily focused on seismic wave propagation in either a single porous layer over a non-homogeneous elastic half-space or in multi-layered media that do not account for surface irregularities. Many of these studies often neglect key characteristics such as porosity, anisotropy, and inhomogeneity, which are critical to understanding wave behavior in complex geological structures. In contrast, this research investigates the propagation of Love waves in a multi-layered medium that includes a fluid-saturated porous layer with a parabolic irregularity at the interface. This approach provides a more comprehensive model that captures the complexities of real-world geological formations. As a result, the findings are more applicable to practical

seismic scenarios. Unlike previous studies that rely on simpler models with homogeneous or perfectly regular interfaces, this study incorporates both non-homogeneity in the half-space and irregularity at the interface. This dual consideration provides a more realistic representation of subsurface conditions typically encountered in natural geological settings. The research builds on well-established foundational models, including Biot's theory of elasticity and perturbation techniques. However, its application to this complex, multilayered system, combined with the inclusion of parabolic interface irregularity, represents a novel extension of existing work. The derived dispersion relation, which links the phase velocity with wave number and irregularity depth, offers new insights. These insights can significantly enhance geophysical interpretations, particularly in regions with irregular geological structures.

The objective of this paper investigates the propagation of Love waves in a multilayered medium with a rigid boundary, consisting a fluid-saturated, transversely isotropic porous layer, positioned between an isotropic layer and a non-homogeneous elastic half-space. The dispersion equation is derived using Biot's theory of elasticity and the Fourier transformation method. Through numerical calculations and computational simulations in MATLAB, this study thoroughly analyzes the influence of key parameters including inhomogeneity, anisotropy, porosity, and the ratio of irregularity depth to layer depth on Love wave propagation.

2 Statement of the problem

To formulate mathematical model for the considered problem, we assume the rectangular coordinate system $(x_1,\ x_2,\ x_3)$ with x_1-axis parallel to the direction of Love wave propagation and x_3-axis oriented vertically downward. The model consists of an isotropic layer of thickness H_2, defined as $(M_1 : -(H_1 + H_2) \leq x_3 \leq -H_1)$, resting over a transversely isotropic fluid-saturated porous layer of depth H_1 $(M_2 : -H_1 \leq x_3 \leq 0)$ over a non-homogeneous elastic half space, defined as $(M_3 : 0 \leq x_3 < \infty)$. The origin 'o' of the coordinate system is located at the midpoint of the irregularity that exists at the interface of porous layer (M_2) and half-space (M_3). The disturbance causing source is positioned on the positive x_3-axes at a distance of $d(d > l)$ from the origin. This configuration is illustrated in the figure below.

The equation for the irregularity considered using Chattopadhyay et al. [28] is.

$x_3 = \varepsilon f(x_1)$, where

$$f(x_1) = \begin{cases} 0, & for\ |x_1| \geq s \\ \frac{2}{s}\left(s^2 - x_1^2\right) & for\ |x_1| < s \end{cases}, \tag{1}$$

where $\varepsilon = \frac{l}{2s} << 1$, $s \neq 0$.

3 Governing equations

The equations of motion for isotropic layer and elastic half space are taken using Ewing's work that describes how waves propagate through an elastic medium. These are second-order partial differential equations that express the balance of forces within the material. The equations of motion for the porous layers were formulated using Biot's theory of elasticity. This theory models the interactions between the fluid and solid phases within the porous medium, capturing both shear and dilatational waves. The constitutive relations for stress and strain were derived separately for each medium, accounting for both fluid-saturated poroelastic properties and the presence of anisotropy. The basic equations for M_1, M_2 and M_3 are given as follows.

3.1 Medium M_1

The dynamical equations of motion in isotropic layer are taken by using Ewing [1], that are as follows

$$\sigma_{ij} = \rho_1 \ddot{u}_i \tag{2}$$

The constitutive relations for M_1 given by Konzack [10] is

$$\sigma_{ij} = \lambda e_{kk}\delta_{ij} + 2\mu e_{ij}, \tag{3}$$

where $e_{ij} = \frac{1}{2}\left(u_{i,\,j} + u_{j,i}\right)$.

As we have considered Love wave propagation x_1x_3-plane, thus displacement vector is independent of x_2-coordinate, that is

$$u_1 = u_3 = 0 \text{ and } u_2 = u_2(x_1, x_3, t) \tag{4}$$

By using Eq. (3)—(4) in Eq. (2), we get

$$\left(\frac{\partial^2}{\partial x_1^2} + \frac{\partial^2}{\partial x_3^2}\right)u_2 + \frac{1}{\mu}\frac{d\mu}{dx_3}\frac{\partial u_2}{\partial x_3} = \frac{1}{c_1^2}\frac{\partial^2 u_2}{\partial t^2} \tag{5}$$

where $c_1^2 = \frac{\mu_1}{\rho_1}$.

3.2 Medium M_2

The dynamical equations of motion in transversely isotropic fluid-saturated porous medium in the absence of the body forces using Biot [29] are

$$\begin{aligned}
&\frac{\partial \tau_{11}}{\partial x_1} + \frac{\partial \tau_{12}}{\partial x_2} + \frac{\partial \tau_{13}}{\partial x_3} = \frac{\partial^2}{\partial t^2}(\rho_{11} v_1 + \rho_{12} V_1) - b_{11}\frac{\partial}{\partial t}(V_1 - v_1),\\
&\frac{\partial \tau_{21}}{\partial x_1} + \frac{\partial \tau_{22}}{\partial x_2} + \frac{\partial \tau_{23}}{\partial x_3} = \frac{\partial^2}{\partial t^2}(\rho_{11} v_2 + \rho_{12} V_2) - b_{12}\frac{\partial}{\partial t}(V_2 - v_2),\\
&\frac{\partial \tau_{31}}{\partial x_1} + \frac{\partial \tau_{32}}{\partial x_2} + \frac{\partial \tau_{33}}{\partial x_3} = \frac{\partial^2}{\partial t^2}(\rho_{11} v_3 + \rho_{12} V_3) - b_{13}\frac{\partial}{\partial t}(V_3 - v_3),\\
&\frac{\partial \tau}{\partial x_1} = \frac{\partial^2}{\partial t^2}(\rho_{12} v_1 + \rho_{22} V_1) + b_{11}\frac{\partial}{\partial t}(V_1 - v_1),\\
&\frac{\partial \tau}{\partial x_2} = \frac{\partial^2}{\partial t^2}(\rho_{12} v_2 + \rho_{22} V_2) + b_{12}\frac{\partial}{\partial t}(V_2 - v_2),\\
&\frac{\partial \tau}{\partial x_3} = \frac{\partial^2}{\partial t^2}(\rho_{12} v_3 + \rho_{22} V_3) + b_{13}\frac{\partial}{\partial t}(V_3 - v_3),
\end{aligned} \tag{6}$$

where $\sigma = -fp$.

The relation between ρ_{11}, ρ_{12}, ρ_{22}, ρ,ρ_s and ρ_f is given by Biot [29], assuming that there is no relative motion between solid and fluid in this medium, that is

$$\begin{aligned}
&\rho_{11} + \rho_{12} = (1-f)\rho_s,\\
&\rho_{11} + \rho_{12} = f\rho_f,\\
&\rho = \rho_s + f(\rho_f - \rho_s).
\end{aligned} \tag{7}$$

The stress–strain relations for the medium M_2 is taken using Konczak [10]

$$\begin{aligned}
\tau_{11} &= (2C_1 + C_2)e_{11} + C_2 e_{22} + C_3 e_{33} + C_6 E,\\
\tau_{22} &= C_2 e_{11} + (2C_1 + C_2)e_{22} + C_3 e_{33} + C_6 E,\\
\tau_{33} &= C_3 e_{11} + C_3 e_{22} + 2C_4 e_{33} + C_7 E,\\
\tau_{23} &= 2C_5 e_{23},\\
\tau_{31} &= 2C_5 e_{31},\\
\tau_{12} &= 2C_1 e_{12},\\
\tau &= C_6 e_{11} + C_6 e_{22} + C_7 e_{33} + C_8 E,
\end{aligned} \tag{8}$$

where

$$\begin{aligned}
e_{ij} &= \frac{1}{2}\left(v_{i,j} + v_{j,i}\right),\\
E &= div V = V_{i,j},\\
e &= div v = v_{k,k}.
\end{aligned} \tag{9}$$

Also, for this medium, we consider

$$\begin{aligned}
&v_1 = v_3 = 0, v_2 = v_2(x_1, x_3, t),\\
&V_1 = V_3 = 0, V_2 = V_2(x_1, x_3, t).
\end{aligned} \tag{10}$$

Using Eq. (8)-(10), the equation of motion in (6) changes to

$$\begin{aligned}
&\frac{\partial^2}{\partial t^2}(\rho_{12} v_2 + \rho_{22} V_2) + b_{11}\frac{\partial}{\partial t}(V_2 - v_2) = 0,\\
&C_1\frac{\partial^2 v_2}{\partial x_1^2} + C_5\frac{\partial^2 v_2}{\partial x_3^2} = \frac{\partial^2}{\partial t^2}(\rho_{12} v_2 + \rho_{22} V_2) + b_{11}\frac{\partial}{\partial t}(V_2 - v_2).
\end{aligned} \tag{11}$$

Eliminating V_2 from above equations gives

$$C_1\frac{\partial^2 v_2}{\partial x_1^2} + C_5\frac{\partial^2 v_2}{\partial x_3^2} - \frac{d\prime}{c_G}\frac{\partial^2 v_2}{\partial t^2} = 0, \tag{12}$$

where $\xi^2 = \frac{(F+iR)}{c_G^2}$, $F = \frac{b_{11}^2+\gamma_{22}\rho^2}{b_{11}^2+\gamma_{22}^2\rho^2}$, $R = \frac{(\gamma_{22}-C*)b_{11}\rho}{b_{11}^2+\gamma_{22}^2\rho^2}$.

Rewriting Eq. (12) by using the substitution $\gamma_{kl} = \frac{\rho_{kl}}{\rho}$; $(k, l = 1, 2)$ (a non-dimensional parameter) as

$$\frac{C_1}{C_5}\frac{\partial^2 v_2}{\partial x_1^2} + \frac{\partial^2 v_2}{\partial x_3^2} - \frac{d\prime}{c_G}\frac{\partial^2 v_2}{\partial t^2} = 0 \tag{13}$$

where $c_G = \sqrt{C_5/\rho}$ is the velocity of Love waves in the corresponding porous layer and $d\prime = \frac{\gamma_{11}\gamma_{22}-\gamma_{12}^2}{\gamma_{22}}$.

3.3 Medium M_3

The dynamical equation of motion for the half-space in absence of the body forces are taken using Ewing [1]

$$t_{ij,j} = \rho^* \ddot{w}_i \tag{14}$$

The constitutive relation given by Konzack [10] is

$$t_{ij} = \lambda p_{kk}\delta_{ij} + 2\mu_3 p_{ij}, \tag{15}$$

where p_{ij} is defined as

$$p_{ij} = \frac{1}{2}\left(w_{i,j} + w_{j,i}\right), p_{kk} = w_{kk} \tag{16}$$

With the help of (15)-(16), and using $w_1 = w_3 = 0$, $w_2 = w_2(x_1, x_3, t)$, Eq. (14) changes to

$$\left(\frac{\partial^2}{\partial x_1^2} + \frac{\partial^2}{\partial x_3^2}\right) w_2 = \frac{1}{c_3^2}\frac{\partial^2 w_2}{\partial t^2} \tag{17}$$

where $c_3^2 = \frac{\mu_3}{\rho_3}$ and

$$\mu_3 = \mu^0 \exp(qx_3), \rho_3 = \rho_0 \exp(qx_3), \tag{18}$$

4 Boundary conditions

The equations of motion are applied to a bounded medium, so specific conditions are introduced to describe the behavior of stresses and displacement at boundaries. These conditions are.

1. At the rigid boundary $x_3 = -H_2$, the displacement components vanishes:

$$u_2(x_1, x_3, t) = 0 \tag{19}$$

2. The interface of medium M_1 and M_2 is continuous that leads the displacement components and stress components to be continuous at $x_3 = -H_1$, i.e.,

   - Continuity of displacement components

$$u_2(x_1, x_3, t) = v_2(x_1, x_3, t) \tag{20}$$

   - Continuity of stress components

$$\sigma_{32} = \tau_{32} \tag{21}$$

3. The interface of medium M_2 and half space M_3 is considered to be continuous that leads the displacement components and stress components to be continuous at $x_3 = \varepsilon f(x_1)$, i.e.,

   - Continuity of displacement components are

$$u_2(x_1, x_3, t) = v_2(x_1, x_3, t) \tag{22}$$

   - Continuity of stress components are

$$C_5\frac{\partial v_2}{\partial x_3} - C_1\varepsilon f'(x_1)\frac{\partial v_2}{\partial x_1} = \mu\left(\frac{\partial w_2}{\partial x_3} - \varepsilon f\prime(x_1)\frac{\partial w_2}{\partial x_1}\right) \tag{23}$$

   where $f\prime(x_1) = \frac{df(x_1)}{dx_1}$.

5 Analytical solution of the problem

The wave is changing harmonically with time, so the solution is assumed in the form

$$\begin{aligned} u_2(x_3,x_1,t) &= u_2^0(x_3,x_1)e^{(i\omega t)},\\ v_2(x_3,x_1,t) &= v_2^0(x_3,x_1)e^{(i\omega t)},\\ V_2(x_3,x_1,t) &= U_2^0(x_3,x_1)e^{(i\omega t)},\\ w_2(x_3,x_1,t) &= w_2^0(x_3,x_1)e^{(i\omega t)} \end{aligned} \tag{24}$$

Using the above Eq. (24), the equations of motion for each medium reduces to

$$\left\{\frac{\partial^2}{\partial x_1^2}+\frac{\partial^2}{\partial x_3^2}+q\frac{\partial^2}{\partial x_3^2}+\frac{\omega^2}{\beta_1^2}\right\}u_2^0=0, \tag{25}$$

$$\left\{\frac{C_{1\prime}}{C_5}\frac{\partial^2}{\partial x_1^2}+\frac{\partial^2}{\partial x_3^2}+\frac{\omega^2}{c_G^2}\right\}v_2^0=0, \tag{26}$$

$$\left\{\frac{C_1}{C_5}\frac{\partial^2}{\partial x_1^2}+\frac{\partial^2}{\partial x_3^2}+\frac{\omega^2}{c_G^2}\right\}V_2^0=0, \tag{27}$$

$$\left\{\frac{\partial^2}{\partial x_1^2}+\frac{\partial^2}{\partial x_3^2}+q\frac{\partial^2}{\partial x_3^2}+\frac{\omega^2}{\beta_3^2}\right\}w_2^0=0. \tag{28}$$

The Fourier transformation and inverse Fourier transformation of the displacement vector are defined as

$$\begin{aligned} \overline{u_2^0}(x_3,\eta) &= \int_{-\infty}^{\infty} u_2^0(x_3,x_1)e^{i\eta x_1}dx_1,\\ u_2^0(x_3,\,x_1) &= \frac{1}{2\pi}\int_{-\infty}^{\infty}\overline{u_2^0}(x_3,\,\eta)e^{-i\eta x_1}d\eta. \end{aligned} \tag{29}$$

Using above Eqs. (25)-(28) reduces to

$$\frac{d^2\overline{u_2^0}}{dx_3^2}+\xi_1^2\overline{u_2^0}=0 \tag{30}$$

$$\frac{d^2\overline{v_2^0}}{dx_3^2}+\xi_2^2\overline{v_2^0}=0 \tag{31}$$

$$\frac{d^2\overline{V_2^0}}{dx_3^2}+\xi_2^2\overline{V_2^0}=0 \tag{32}$$

$$\frac{d^2\overline{w_2^0}}{dx_3^2}-\xi_3^2\overline{w_2^0}=0 \tag{33}$$

where

$$\begin{aligned} \xi_1^2 &= \left(\frac{\omega^2}{\beta_1^2}-\eta^2\right),\\ \xi_2^2 &= \frac{C_1}{C_5}\left(\eta^2-\frac{d\omega^2}{c_G^2}\right),\\ \xi_3^2 &= \left(\frac{\omega^2}{\beta_3^2}-\eta^2\right). \end{aligned} \tag{34}$$

The general solution of the differential Eqs. (30–33) is represented as

$$\overline{u_2^0} = D\cos(\xi_1 x_3)+E\sin(\xi_1 x_3), \tag{35}$$

$$\overline{v_2^0} = F\cos(\xi_2 x_3)+G\sin(\xi_2 x_3), \tag{36}$$

$$\overline{V_2^0} = \overline{F}\cos(\xi_2 x_3)+\overline{G}\sin(\xi_2 x_3), \tag{37}$$

$$\overline{w_2^0} = J\exp(-\xi_3 x_3),\ \sin ce\, 0 \le z < \infty \tag{38}$$

where D, E, F, G, $\overline{F}$, $\overline{G}$ and J are any arbitrary functions of η.

From the inverse Fourier transformation defined in Eq. (29), Eqs. (35)—(38) simplified to

$$u_2^0(x_3,x_1) = \frac{1}{2\pi}\int_{-\infty}^{\infty}(D\cos(\xi_1 x_3) + E\sin(\xi_1 x_3))e^{-i\eta x_3}d\eta \tag{39}$$

$$v_2^0(x_3,x_1) = \frac{1}{2\pi}\int_{-\infty}^{\infty}(F\cos(\xi_2 x_3) + G\sin(\xi_2 x_3))e^{-i\eta x_1}d\eta \tag{40}$$

$$V_2^0(x_3,x_1) = \frac{1}{2\pi}\int_{-\infty}^{\infty}\left(\overline{F}\cos(\xi_2 x_3) + \overline{G}\sin(\xi_2 x_3)\right)e^{-i\eta x_1}d\eta \tag{41}$$

$$w_2^0(x_3,x_1) = \frac{1}{2\pi}\int_{-\infty}^{\infty}\left(Je^{-\xi_3 x_3} + \frac{2}{\xi_3}e^{-\xi_3 x_3}e^{\xi_3 d}\right)e^{-i\eta x_1}d\eta. \tag{42}$$

In Eq. (42) a second term, $\left(\frac{2}{\xi_3}e^{-\xi_3 x_3}e^{\xi_3 d}\right)$, is added in the integrand to represent the presence of disturbance causing source that is placed at a distance of d from origin on positive x_3-axis in the half-space.

To simplify the problem, we applied Fourier transformation to Eqs. (25)-(28). This transformation converted the partial differential equations governing the wave propagation into ordinary differential equation in algebraic forms, allowing for easier manipulation and integration. The inverse Fourier transformation was then used to recover the physical displacement fields from the frequency domain solutions.

Following the perturbation method by Eringen and Samuels [30] the arbitrary functions D, E, F, G, and J can be set using a small positive constant ε, as

$$\begin{aligned}
&D \cong D_0 + D_1\varepsilon,\ E \cong E_0 + E_1\varepsilon,\\
&F \cong F_0 + F_1\varepsilon,\ G \cong G_0 + G_1\varepsilon,\\
&J \cong J_0 + J_1\varepsilon,\ e^{\pm\alpha\varepsilon f} \cong 1 \pm \alpha\varepsilon f,\\
&\cos(\xi_1\varepsilon f) \cong 1,\ \sin(\xi_1\varepsilon f) \cong \xi_1\varepsilon f,
\end{aligned} \tag{43}$$

Fourier transformation and inverse Fourier transformation for $f(x_1)$ is

$$\overline{f}(\lambda) = \int_{-\infty}^{\infty} f(x_1)e^{i\lambda x_1}d\lambda \tag{44}$$

$$f(x_1) = \frac{1}{2\pi}\int_{-\infty}^{\infty}\overline{f}(\lambda)e^{-i\lambda x_1}d\lambda. \tag{45}$$

Therefore

$$f\prime(x_1) = \frac{-i}{2\pi}\int_{-\infty}^{\infty}\lambda\overline{f}(\lambda)e^{-i\lambda x_1}d\lambda. \tag{46}$$

6 Frequency relation

The displacement components as given in Eqs. (35)-(38) along with (43) can be simplified to a system of ten non-homogenous linear equation using the boundary conditions from Eqs. (19) and (21) in equation and Fourier transformation for $f(x_1)$ in Eq. (45)-(46)

$$\begin{aligned}
&D_0\cos(\xi_1(H_1+H_2)) - E_0\sin(\xi_1(H_1+H_2)) = 0,\\
&D_0\cos\xi_1 H_2 - E_0\sin\xi_1 H_2 - F_0\cos\xi_2 H_2 + J_0\sin\xi_2 H_2 = 0,\\
&\mu_1\xi_1(D_0\sin\xi_1 H_2 + E_0\cos\xi_1 H_2) - C_5\xi_2(F_0\sin\xi_2 H_2 + G_0\cos\xi_2 H_2) = 0,\\
&F_0 - J_0 = \frac{2}{\xi_3}e^{-\xi_3 d},\\
&\mu_1\xi_1 J_0 + C_5\xi_2 J_0 = 2\mu_0 e^{-\xi_3 d},\\
&D_1\cos(\xi_1(H_1+H_2)) - E_1\sin(\xi_1(H_1+H_2)) = 0,\\
&D_1\cos\xi_1 H_2 - E_1\sin\xi_1 H_2 - F_1\cos\xi_2 H_2 + J_1\sin\xi_2 H_2 = 0,\\
&\mu_1\xi_1(D_1\sin\xi_1 H_2 + E_1\cos\xi_1 H_2) - C_5\xi_2(F_1\sin\xi_2 H_2 + G_1\cos\xi_2 H_2) = 0,\\
&J_1 - F_1 = W_1(k),\\
&\mu_3\xi_3 J_1 + C_5\xi_2 G_1 = W_2(k),
\end{aligned} \tag{47}$$

where

$$W_1(k) = \frac{1}{2\pi}\int_{-\infty}^{\infty}(B_0\xi_1 - \xi_3 D_0 + 2e^{-\xi_3 d})^{\eta=k-\lambda} f(\lambda)d\lambda. \tag{48}$$

$$W_2(k) = \frac{1}{2\pi}\int_{-\infty}^{\infty}\left[\xi_1^2 C_5 A_0 - \mu_0\left(\xi_3^2 D_0 + 2\xi_3 e^{-\xi_3 d}\right) - \mu_0\lambda k\xi_3\left(D_0 - \frac{2}{\xi_3}e^{-\xi_3 d}\right)^{\eta=k-\lambda} f(\lambda)d\lambda\right] \tag{49}$$

The perturbation method is employed to handle the complexity introduced by the parabolic irregularity at the interface and the boundary conditions. This technique allowed for the approximation of the solution by introducing a small parameter ε and expanding the displacement field in terms of this parameter.

Solving the above set of equations, we obtain the values of unknowns as

$$D_0 = \frac{8\mu_3 C_5\xi_2 e^{-\xi_1 d}\tan(H_1+H_2)\left(1+\tan^2\xi_2 H_2\right)}{\Delta(k)},$$

$$E_0 = \frac{4\mu_3 C_5\xi_2 e^{-\xi_3 d}\left(1+\tan^2\xi_2 H_2\right)}{\Delta(k)},$$

$$F_0 = \frac{4\mu_3 e^{-\xi_3 d}}{\Delta(k)}\begin{bmatrix}\mu_3\xi_1\tan\xi_2 H_2(1+\tan\xi_1 H_2\tan\xi_1(H_1+H_2))\\ +C_5\chi_2(\tan\xi_1 H_2 - \tan\xi_1(H_1+H_2))\end{bmatrix},$$

$$G_0 = \frac{4\mu_3 e^{-\xi_3 d}}{\Delta(k)}\begin{bmatrix}\mu_3\xi_1(1+\tan\xi_1 H_2\tan\xi_1(H_1+H_2))\\ -C_5\xi_2\tan\xi_2 H_2(\tan\xi_1(H_1+H_2) - \tan\xi_1 H_2)\end{bmatrix},$$

$$J_0 = \frac{2\mu_3 e^{-\xi_3 d}}{\Delta(k)}\begin{bmatrix}(C_5\xi_3+\mu_3\xi_1)(\mu_3\xi_1 - C_5\xi_3)\tan\xi_1(H_1+H_2)\\ +(C_5\xi_2+\mu_3\xi_1)(\mu_3\xi_1 - C_5\xi_2)\tan\xi_1 H_2\end{bmatrix},$$

$$D_1 = \frac{(W_2 - \mu_3\xi_3 W_1)C_5\xi_2}{\Delta(k)}\left[\left(1+\tan^2\xi_2 H_2\right)\tan\xi_1(H_1+H_2)\right],$$

$$E_1 = \frac{(W_2 - \mu_3\xi_3 W_1)C_5\xi_2\left(1+\tan^2\xi_2 H_2\right)}{\Delta(k)},$$

$$F_1 = \frac{(W_2 - \mu_3\xi_3 W_1)}{\Delta(k)}\begin{bmatrix}\mu_3\xi_1(W_2\tan\xi_1 H_2\\ (1+\tan\xi_1 H_2\tan\xi_1(H_1+H_2))\\ +C_5\xi_1(\tan\xi_1 H_2 - \tan\xi_1(H_1+H_2))\end{bmatrix},$$

$$G_1 = \frac{(W_2 - \mu_3\xi_3 W_1)}{\Delta(k)}\begin{bmatrix}\mu_3\xi_1(1+\tan\xi_1 H_2\tan\xi_1(H_1+H_2))\\ +C_5\xi_2\tan\xi_2 H_2(\tan\xi_1 H_2 - \tan\xi_1(H_1+H_2))\end{bmatrix},$$

$$J_1 = \frac{1}{\Delta(k)}\begin{bmatrix}\mu_1\xi_1(W_2\tan\xi_2 H_2 + W_1 C_5\xi_2)(1+\tan\xi_1 H_2\tan\xi_1(H_1+H_2))\\ +C_5\xi_2(W_2 - C_5\xi_2 W_1\tan\xi_2 H_2)(\tan\xi_1(H_1+H_2) - \tan\xi_1 H_2)\end{bmatrix} \tag{50}$$

where $\Delta(k)$ is defined as

$$\Delta(k) = \begin{bmatrix}\mu\chi_1(1+\tan\chi_1 H_2\ \tan\ \chi_1(H_1+H_2))(\mu\chi_3\tan\chi_2 H_2 + C_5\chi_2)\\ +C_5\chi_2(\tan\chi_1(H_1+H_2) - \tan\chi_1 H_2)(C_5\chi_2\tan\chi_2 H_2 - \mu\chi_3)\end{bmatrix} \tag{51}$$

The displacement vector of porous layer, v_2^0, in Eq. (40) changes to

$$v_2^0 = \frac{1}{2\pi}\int_{-\infty}^{\infty}\left(\frac{4\mu_3 e^{-\xi_3 d}}{\Delta(k)}\left[1 + \frac{\varepsilon(W_2 - \mu_3\xi_3 W_1)e^{\xi_3 d}}{4\mu_3}\right][S_1+S_2]e^{-ikx_1}\right)dk \tag{52}$$

where

$$S_1 = \mu_3\xi_1(1+\tan(\xi_1 H_2)\tan\xi_1(H_2+H_1))(\sin(\xi_2 x_3) + \tan\xi_2 H_2\cos(\xi_2 x_3))$$

$$S_2 = C_5\xi_2(\tan(\xi_1(H_1+H_2) - \tan\xi_1 H_2)(\cos\xi_2 x_3 - \tan\xi_2 H_2\sin\xi_2 x_3)$$

From the equation of irregularity (1) and its Fourier transformation, we get

$$f(\lambda) = \frac{4}{\lambda^3}\sin(\lambda s) - \frac{4s}{\lambda^2}\cos(\lambda s). \tag{53}$$

Using Eqs. (48)—(49), along with (53) we have

$$W_2 - \mu_3\xi_3 W_1 = \frac{8s\mu_3}{\pi}\int_0^{\infty}\frac{1}{\lambda^2}[g(k-\lambda) + g(k+\lambda)]\left[\frac{1}{\lambda}\sin(\lambda s) - 4\cos(\lambda s)\right]d\lambda \tag{54}$$

where

$$g(k-\lambda) = (A_2 + A_3)$$

$$A_2 = D_0\xi_1^2 C_5 - \mu_3\xi_3\left(\xi_1 E_0 - 4e^{-\xi_3 d}\right) \tag{55}$$

$$A_3 = -\lambda k\left(\mu_3\xi_3 D_0 - 2\mu_3 e^{-\xi_3 d}\right) \tag{56}$$

Now, using the asymptotic formula given by Willis [31] and Tranter [32], solve the integral in Eq. (54) and ignore the terms containing $2/s$ and its higher powers, since s is very large

$$\int_0^\infty \frac{1}{\lambda^2}[g(k-\lambda)+g(k+\lambda)]\left[\frac{1}{\lambda}\sin(\lambda s) - 4\cos(\lambda s)\right]d\lambda = \frac{\pi}{2}.2g(k) = \pi g(k) \tag{57}$$

Thus, from Eq. (57), Eq. (54) becomes

$$W_2 - \mu_3\xi_3 W_1 = \frac{8l\mu_3}{\varepsilon}g(k) \tag{58}$$

The displacement vector of porous isotropic layer in Eq. (52) becomes

$$v_2^0 = \frac{1}{\pi}\int_{-\infty}^{\infty}\left(\frac{4\mu_3 e^{-\xi_3 d}}{\Delta(k)\left[1 - lg(k)e^{\xi_3 d}\right]}[S_1 + S_2]e^{-ikx_1}\right)dk \tag{59}$$

The value of integral in Eq. (59) depends entirely on the contribution of poles of the integrand. Therefore, the dispersion equation is given by the roots of equation

$$E(k)[1 - H_1 g(k)e^{\xi_3 d}] = 0 \tag{60}$$

By solving Eq. (60) and equating the real parts we get the dispersion equation for Love waves, as

$$\begin{aligned}&\frac{\mu P_1}{C_5 P_2}\left(1 + \tan(P_1 k H_1)\tan(P_1 k(H_1+H_2))\left[\begin{matrix}(1 - P_1 kl)(C_5 P_2 + \mu_3 P_3 \tan k H_1)\\ -l P_2 k(C_5 P_2 \tan P_2 k H_2 - \mu_3 P_3 k H_1)\end{matrix}\right]\right)\\ &= [\tan(P_1 k(H_1+H_2)) - \tan(P_1 k H_1)][(1 - P_1 kl)(C_5 P_2 + \mu P_3 \tan k H_1) + l P_2 k(C_5 P_2 \tan P_2 k H_2 - \mu_3 P_3 k H_1)]\end{aligned} \tag{61}$$

where,

$$P_1 = \sqrt{1 - \frac{c^2}{c_1^2}} \tag{62}$$

$$P_2 = \sqrt{\frac{c^2}{C_G^2} - \frac{C_1}{C_5}} \tag{63}$$

$$P_3 = \sqrt{1 - \frac{c^2}{c_3^2}} \tag{64}$$

and $c \le c_1$, $c \le c_3$.

The obtained dispersion equation of Love waves describes the properties of the wave, the medium and the effect of various factors on the waves.

The combination of Fourier transformation and perturbation techniques led to the derivation of the dispersion equation, which links the phase velocity of the Love wave to the wave number and various factors of the model. The boundary conditions at the interface between the isotropic, porous, and elastic half-space layers were applied to ensure continuity of displacement and stress fields across the layers.

7 Particular cases

Some specific cases for the considered problem are discussed as follows:

Case 1: when the layer M_1 is omitted, so that the model consists of porous layer M_2 over the nonhomogeneous half space M_3 only, by substituting $H_2 = 0$ in Eq. (58) it is simplified to

$$\tan(P_2 k H_1) = \frac{\mu P_3 + \mu P_3^2 kl - l P_2^2 k C_5}{\mu P_2 P_3 lk + \mu_2 P_2 + P_3 kl C_5 P_2} \tag{65}$$

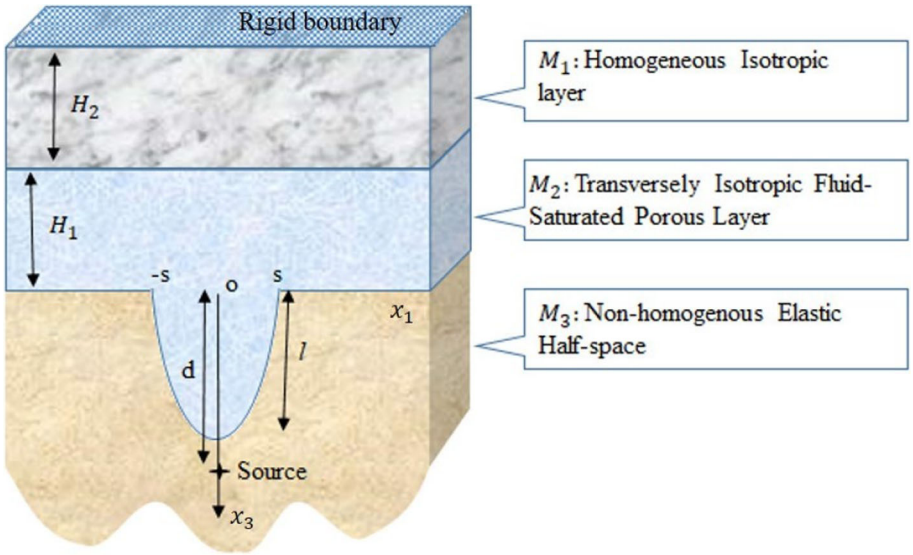


Fig. 1 Geometry of the Problem

Case 2: when the irregularity at the interface is removed (by considering $l = 0$) in case 1, Eq. (65) changes to

$$\tan(P_2 k H_1) = \frac{\mu_3 P_3}{\mu_2 P_2} \tag{66}$$

Substituting values of P_2 and P_3 in Eq. (66), it becomes

$$\tan\left(kH_1\sqrt{\frac{c^2}{C_G^2} - \frac{C_1}{C_5}}\right) = \frac{\mu_3\sqrt{1 - \frac{c^2}{c_3^2}}}{\mu_2\sqrt{\frac{c^2}{C_G^2} - \frac{C_1}{C_5}}} \tag{67}$$

This equation represents the classical dispersion equation for Love waves obtained by Love [35].

8 Numerical discussions

This section explores the impact of different factors on the phase velocity of Love waves using the dispersion relation in Eq. (61). The numerical computation has been carried out using the data by Gubbins [2] and Ding et al. [33].

$$\mu_1 = 7.45 \times 10^{10}\, N/m^2,$$

$$\rho_{11} = 3321\, kg/m^3,\ \rho_{12} = 2802\, kg/m^3,$$
$$\rho_{22} = 3293\, kg/m^3,\ \rho = 2543\, kg/m^3,$$
$$C_5 = 9.4 \times 10^{10}\, N/m^2,$$
$$\mu_3 = 7.84 \times 10^{10}\, N/m^2.$$

This section is divided in three subsections, first subsection describes the effect of inhomogeneity parameter (q) on phase velocity of Love waves in two cases, first in the absence of upper layer, i.e., ($H_2 = 0$), second in the absence of porous layer, i.e., ($H_1 = 0$). Second subsection describes the impact of porosity of porous layer (M_2) on phase velocity of Love waves. Third subsection describes the impact of anisotropy factor of porous layer (M_2) on phase velocity of Love waves.

8.1 Effect of inhomogeneity parameter

Figure 1, 2, 3, 4 and 5 show the variation of dimensionless phase velocity of Love wave against wave number (kH_1) in the absence of M_1, for $q = 0,\ 1,\ 2,\ 3$. The curves in each figures represent phase velocity for different ratio of depth of irregularity to width of porous layer, i.e., $l/H_1 = 0.10,\ 0.20,\ 0.30,\ 0.40$, respectively, these curves shows the pattern that whenever the wave number is increasing the non-dimensional phase velocity is decreasing. Each figure represents that the phase velocity is diminishing with the increment in ratio l/H_1.

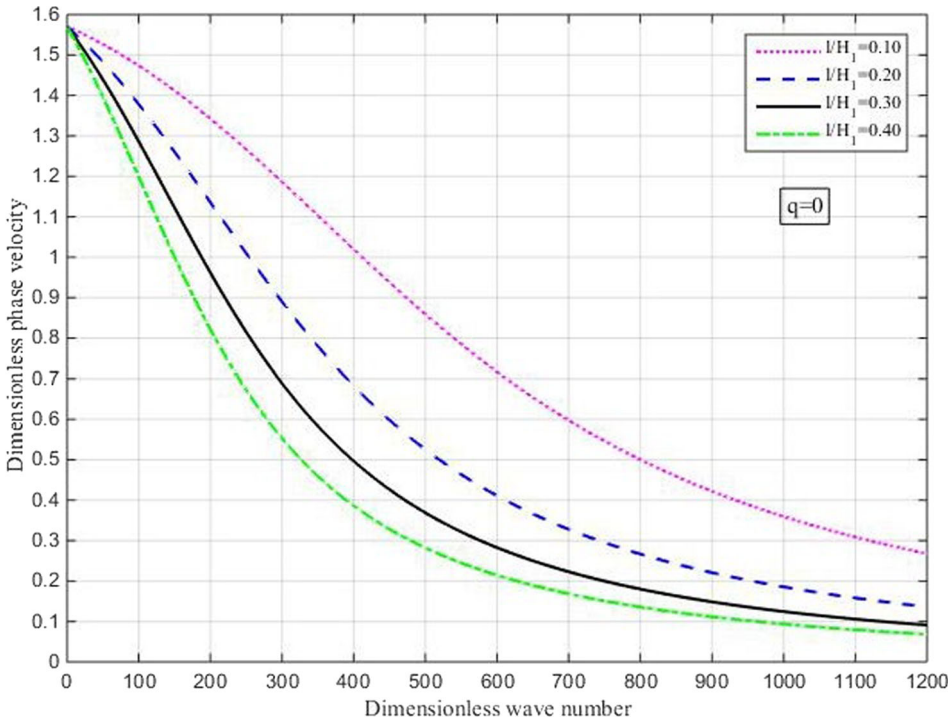


Fig. 2 Phase velocity (c/c_G) versus wave number (kH_1) for inh omogeneity parameter $q = 0$

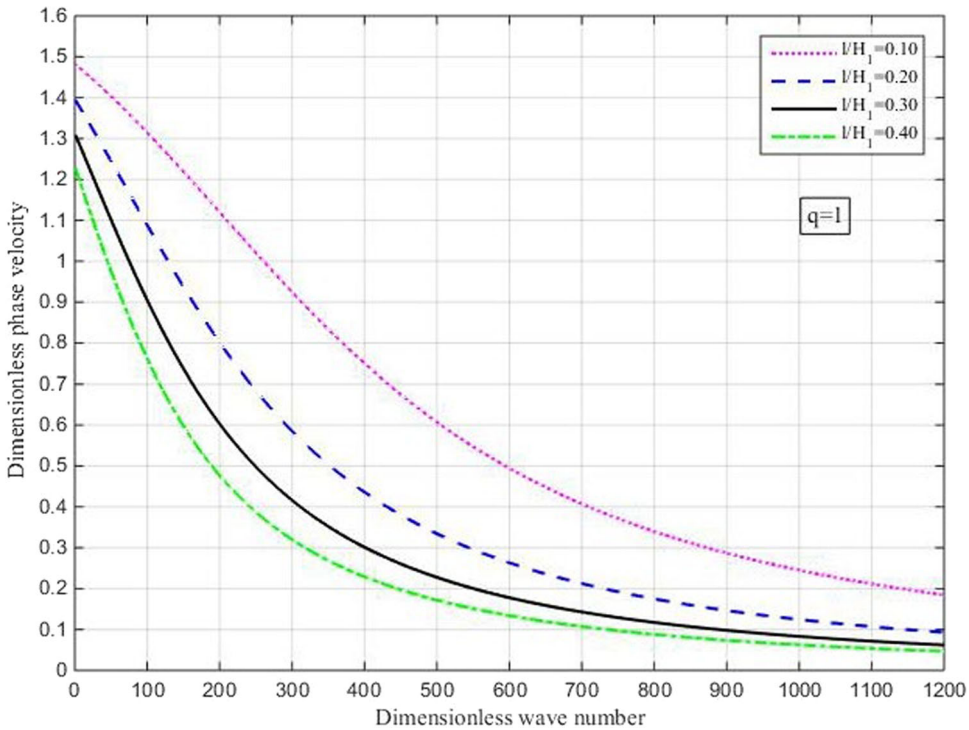


Fig. 3 Phase velocity (c/c_G) versus wave number (kH_1) for inhomogeneity parameter $q = 1$

Figure 6, 7, 8 and 9 show the variation of dimensionless phase velocity of Love wave against wave number (kH_2) in the absence of medium M_2, for $q = 0, 1, 2, 3$. These figures show the similar pattern that as the wave number is increasing the non-dimensional phase velocity is decreasing monotonically and tending to 0 for higher value of wave number.

8.2 Effect of anisotropy factor

In Figs. 10 and 11, the anisotropy effect of M_2 on the dimensionless phase velocity versus dimensionless wave number curve is represented for homogenous half-space $(q = 0)$ with $C_1/C_5 = 0.1$ and 0.2 and Fig. 12- Fig. 13 shows this variation for nonhomo-

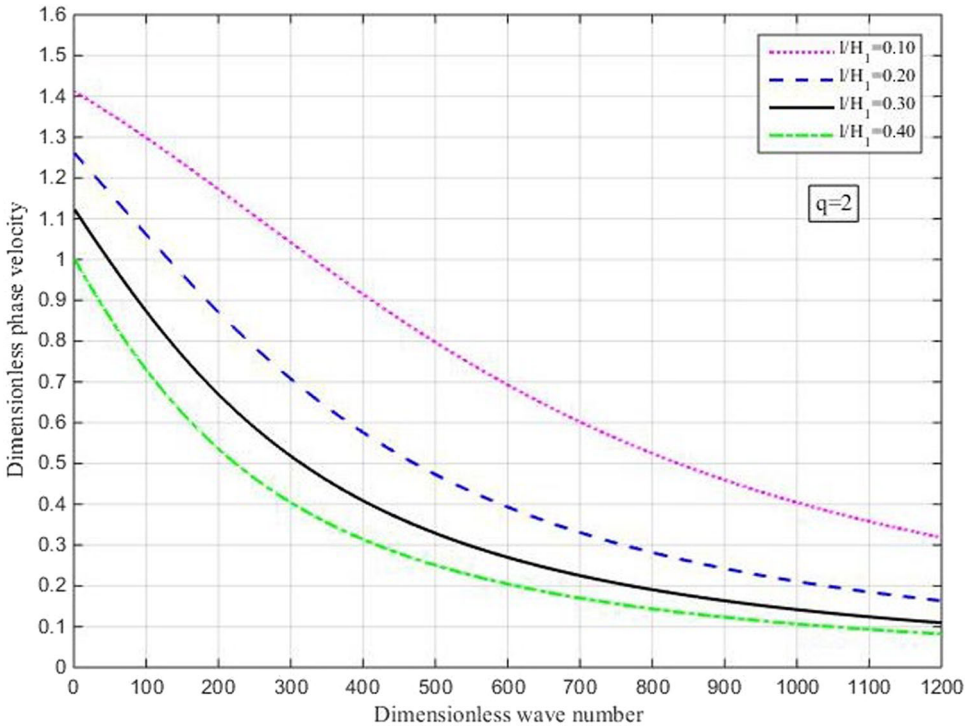


Fig. 4 Phase velocity (c/c_G) versus wave number (kH_1) for inhomogeneity parameter $q = 2$

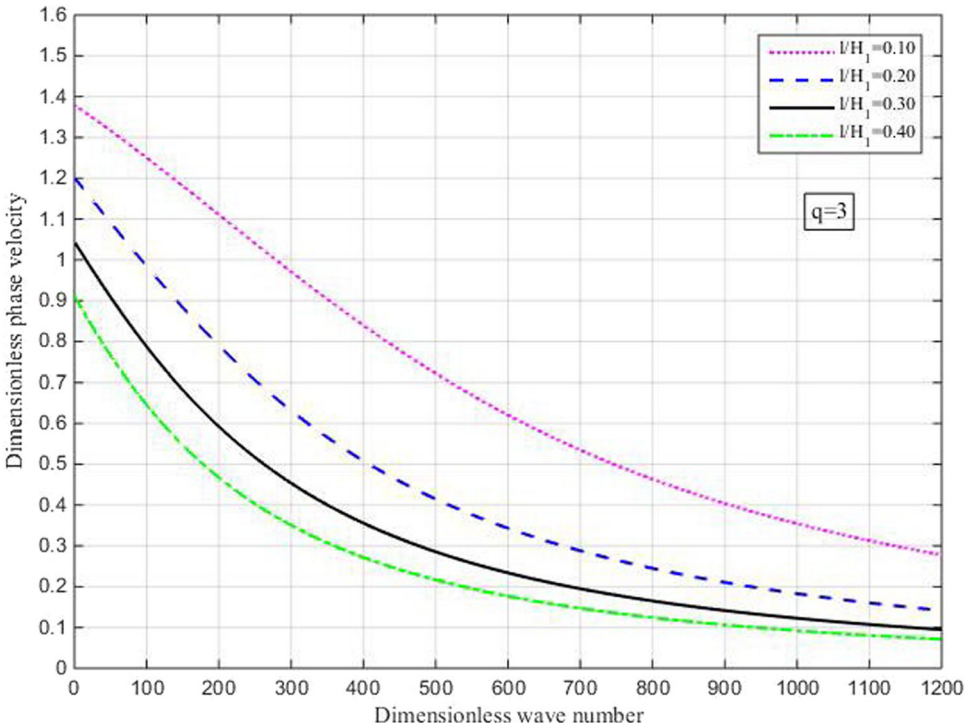


Fig. 5 Phase velocity (c/c_G) versus wave number (kH_1) for inhomogeneity parameter $q = 3$

geneous half-space ($q = 1$) with $C_1/C_5 = 0.1$ and 0.2. In this analysis the ratio of height of first layer (M_1) to the height of second layer (M_2) is considered as $H_2/H_1 = 0.5$. These figures show that whenever the anisotropy ratio is increasing, the magnitude of phase velocity is decreasing proportionally. By comparing Figs. 10 and 11 with Figs. 12–13, this is observed that with the increment in q, the magnitude of phase velocity is decreasing slightly, while all the figures show the pattern that as the wave number rises, phase velocity of Love wave diminishes. The anisotropy factor is varied between 0.1 and 0.2 for homogeneous and nonhomogeneous half-space cases. These values align with anisotropic behaviors commonly found in geological formations, and the linear decrease in phase velocity with increasing anisotropy holds true across this range.

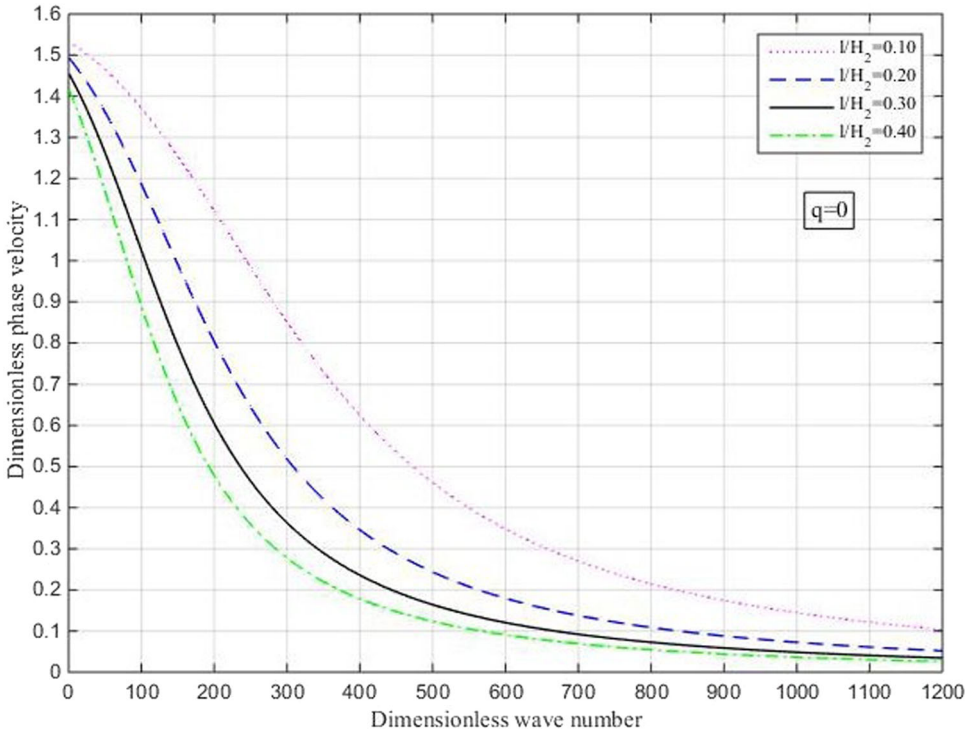


Fig. 6 Phase velocity (c/c_G) versus wave number (kH_2) for inhomogeneity parameter $q = 0$

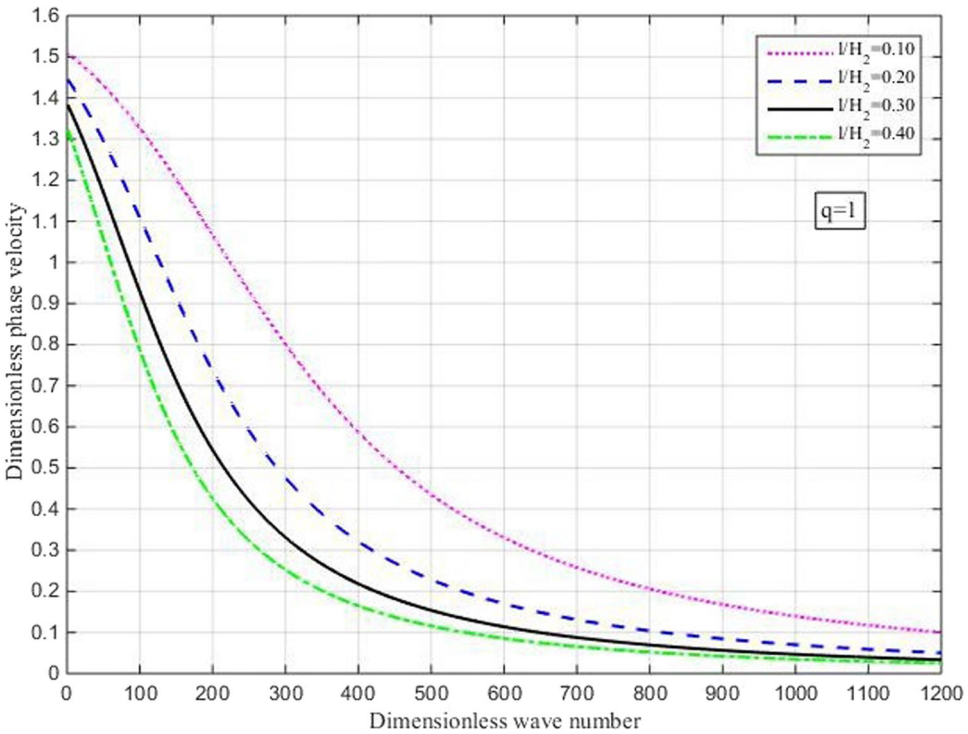


Fig. 7 Phase velocity (c/c_G) versus wave number (kH_2) for inhomogeneity parameter $q = 1$

8.3 Effect of porosity

In Figs. 14 and 15, the porosity effect of M_2 is represented on the dimensionless phase velocity versus dimensionless wave number curves for homogenous half-space ($q = 0$) with $f = 1.2$ and 1.4, whereas Figs. 16, 17 show this variation for non-homogenous half-space ($q = 1$) with $f = 1.2$ and 1.4. The curves in each figure represent the different ratio for l/H_1, and the ratio of the medium's height is considered to be $H_2/H_1 = 0.5$. Figures 14, 17 show that whenever the porosity is increasing, the magnitude of phase velocity is decreasing, along with the increment in inhomogeneity parameter q, while all the figures show that the phase

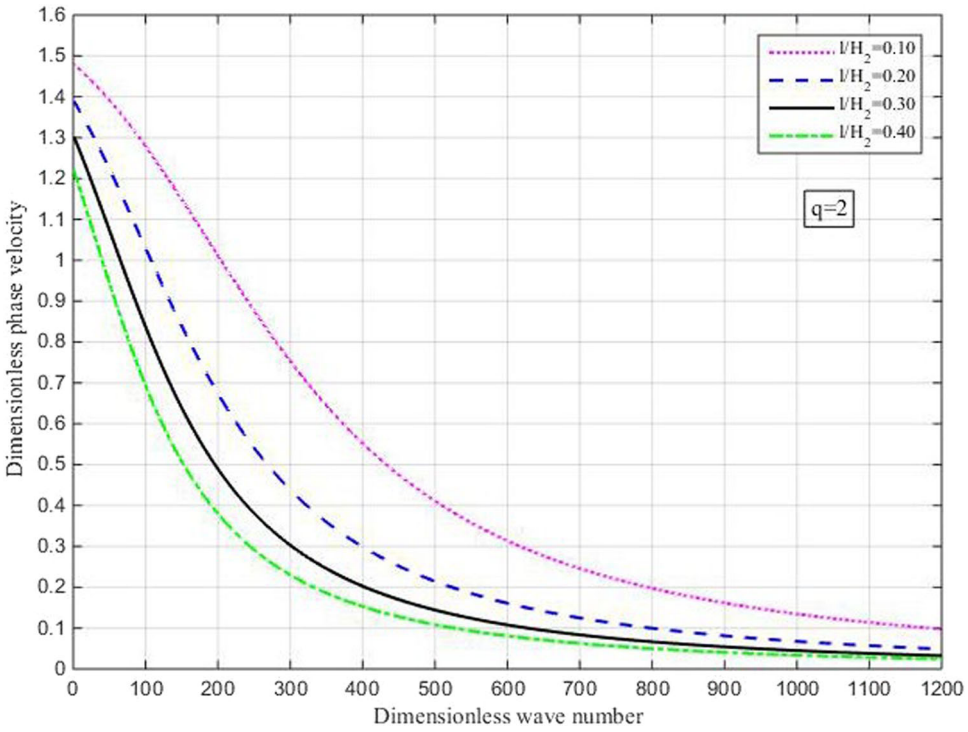


Fig. 8 Phase velocity (c/c_G) versus wave number (kH_2) for inhomogeneity parameter $q = 2$

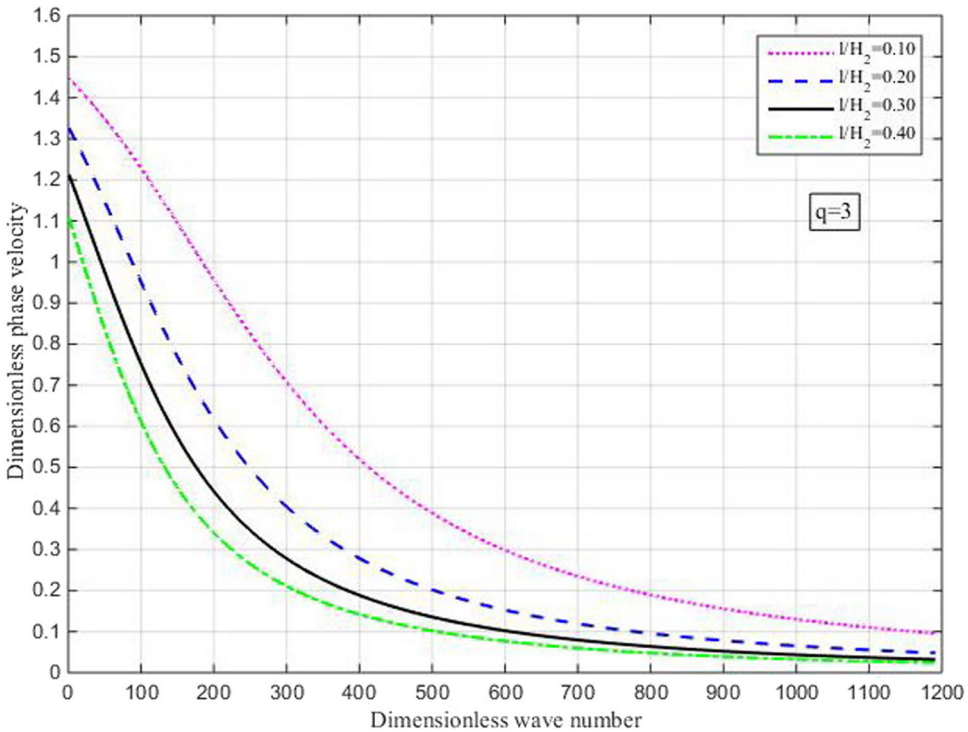


Fig. 9 Phase velocity (c/c_G) versus wave number (kH_2) for inhomogeneity parameter $q = 3$

velocity diminishes with the rise in the wave number. The porosity factor is varied between 1.2 and 1.4 for homogeneous and nonhomogeneous half space, representing realistic values for fluid-saturated porous layers. The trends observed in phase velocity are consistent within this range.

The trends observed in the figures, where phase velocity decreases with increasing wave number, anisotropy, and porosity, can be explained based on the physical interactions between the fluid and solid matrices and the material properties of the medium. As the wave number increases, the shorter wavelength interacts more strongly with the internal structures of the medium, leading to increased scattering and energy dissipation. Similarly, increasing anisotropy introduces directional stiffness variations, when

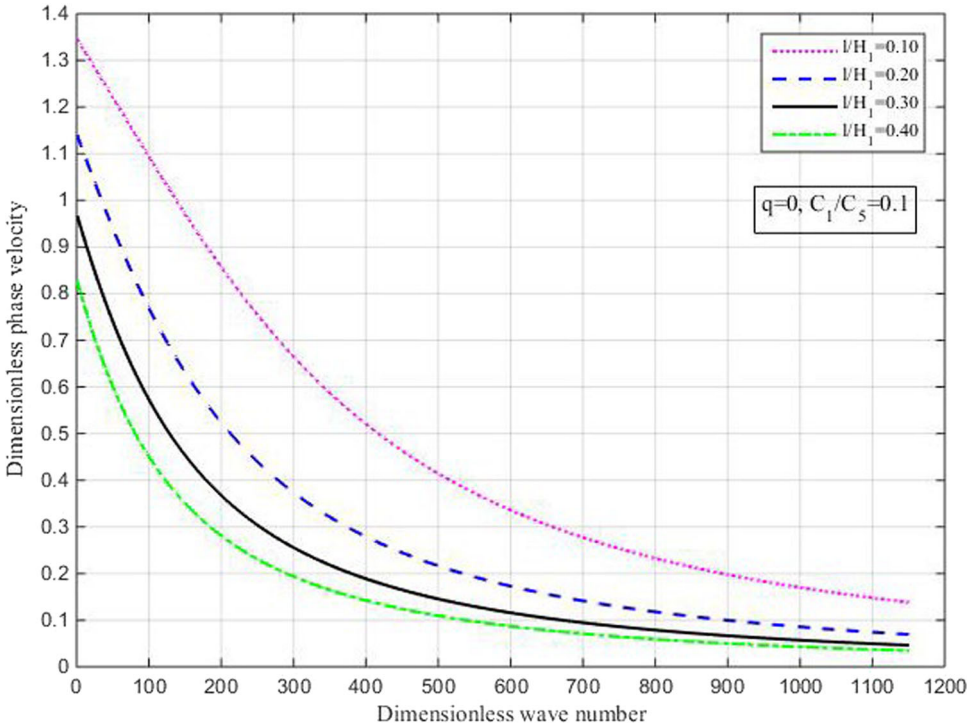


Fig. 10 Phase velocity versus wave number for inhomogeneity parameter $q = 0$ and porosity factor $C_1/C_5 = 0.1$

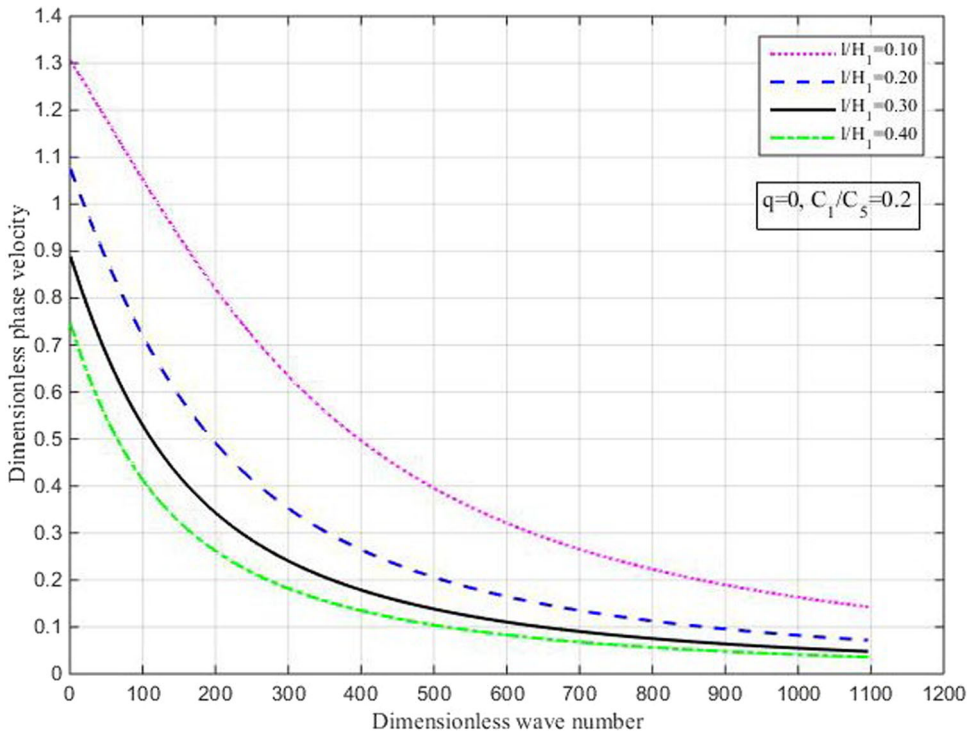


Fig. 11 Phase velocity versus wave number for inhomogeneity parameter $q = 0$ and porosity factor $C_1/C_5 = 0.2$

anisotropy increases, the medium becomes less uniform in its ability to transmit waves, leading to slower wave speeds in certain directions due to weaker elastic properties along those axes. Increasing porosity weakens the solid matrix and increases fluid–solid interaction, both of which reduce the medium's ability to support Love waves, resulting in lower phase velocities.

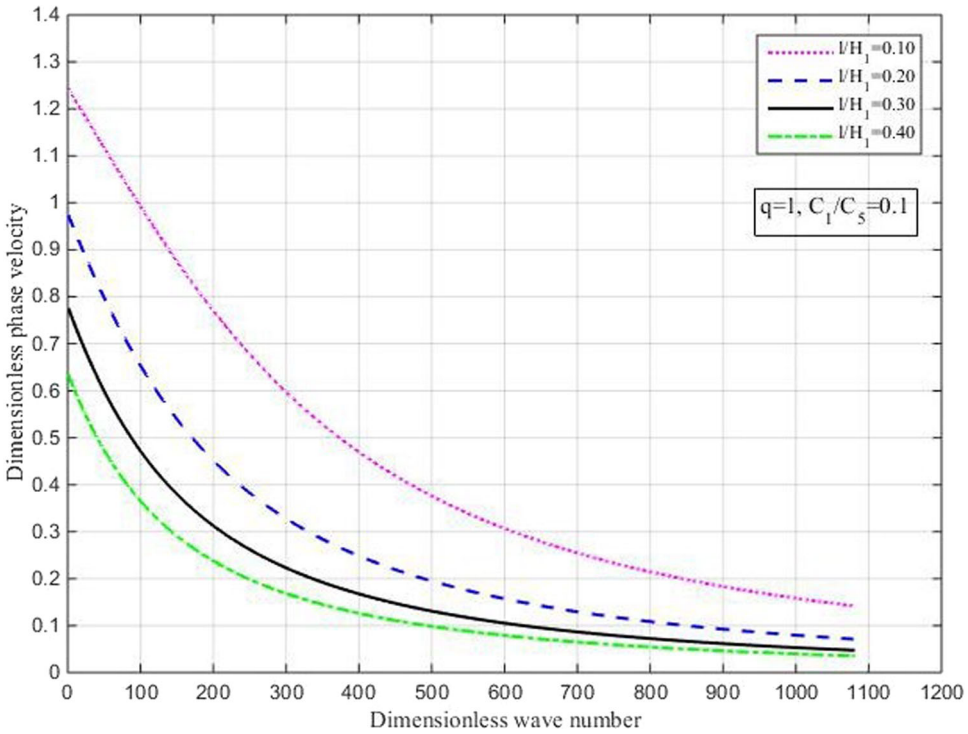


Fig. 12 Phase velocity versus wave number for inhomogeneity parameter $q = 1$ and porosity factor $C_1/C_5 = 0.1$

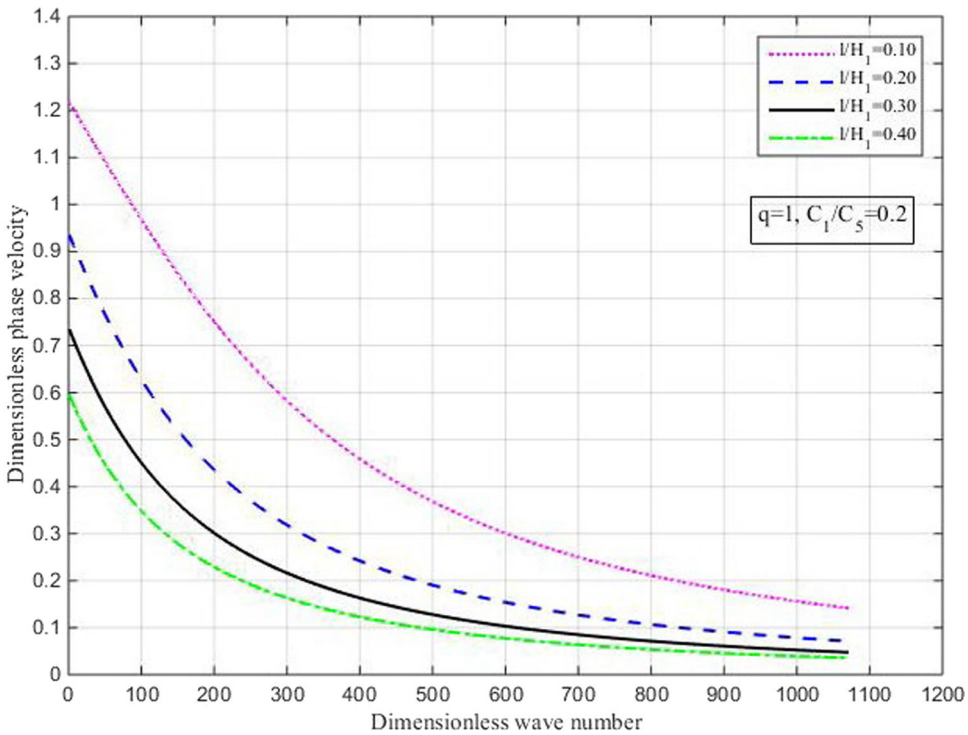


Fig. 13 Phase velocity versus wave number for inhomogeneity parameter $q = 1$ and porosity factor $C_1/C_5 = 0.2$

9 Simulation details

In this research work, the numerical method was implemented using custom MATLAB code, with no reliance on external packages for the graphical computations. The figures in Fig. 2- Fig. 17 were generated using MATLAB's built-in 'plot' and 'legend' functions. The mesh 2D plots employed in the simulations are generated using the plot function only.

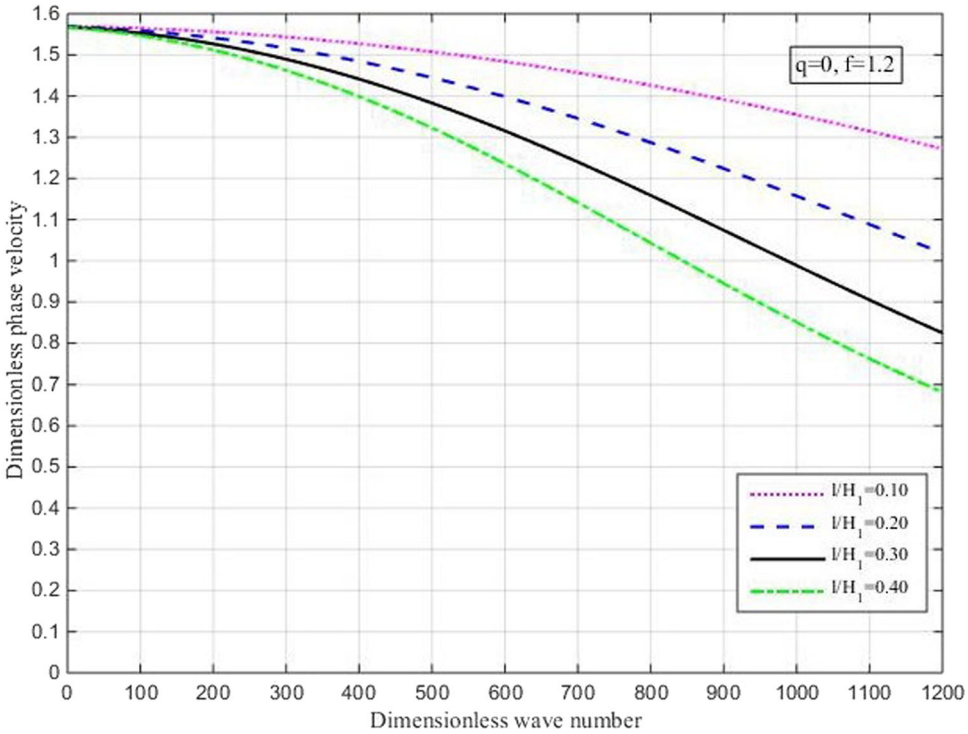


Fig. 14 Phase velocity (c/c_G) versus wave number (kH_2) for inhomogeneity parameter $q = 0$ and porosity factor $f = 1.2$

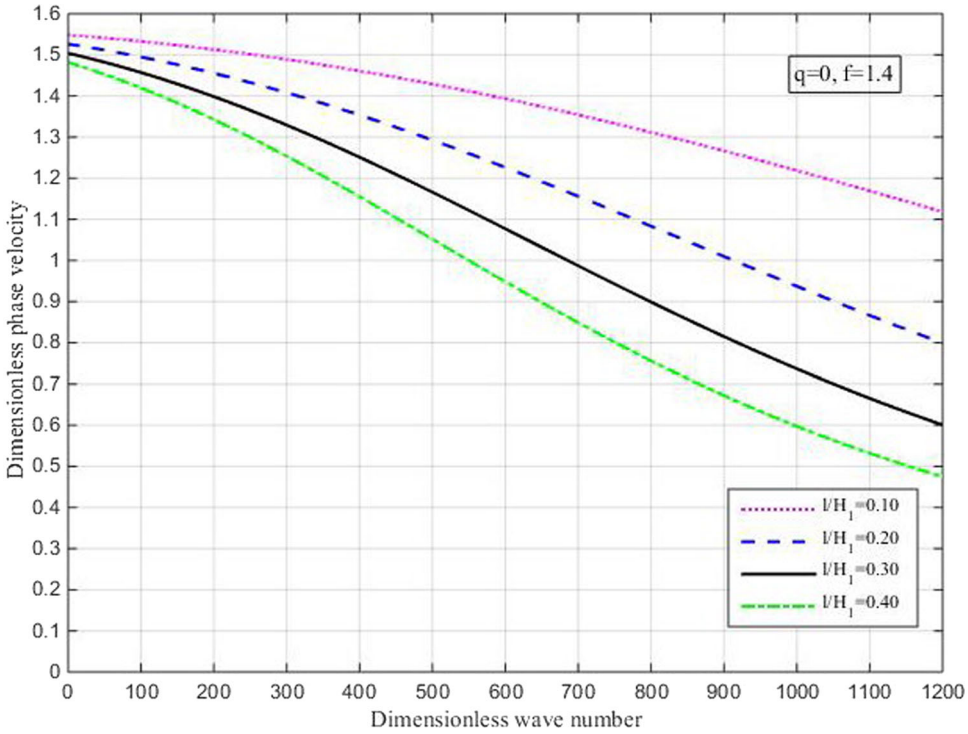


Fig. 15 Phase velocity (c/c_G) versus wave number (kH_2) for inhomogeneity parameter $q = 0$ and porosity factor $f = 1.4$

The approximate CPU time for each simulation was calculated by recording the start time with "tStart = cputime;" at the beginning of each code and the end time "tEnd = cputime – tStart" at the end. The CPU hours for each simulation are presented in the table as follows: Table. 1

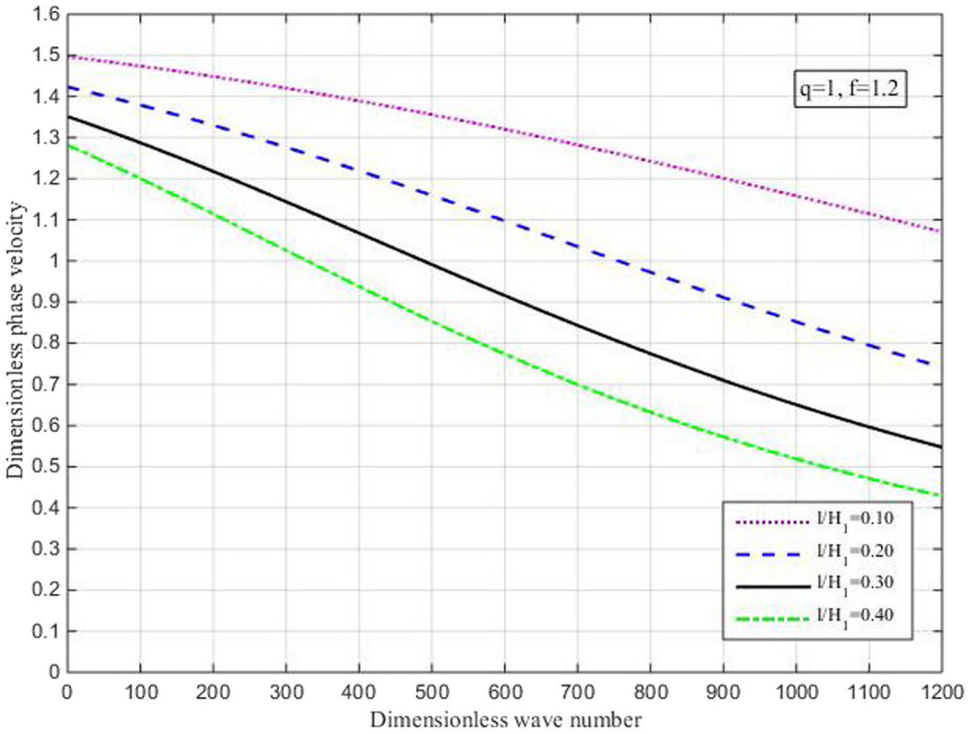


Fig. 16 Phase velocity (c/c_G) versus wave number (kH_2) for inhomogeneity parameter $q = 1$ and porosity factor $f = 1.2$

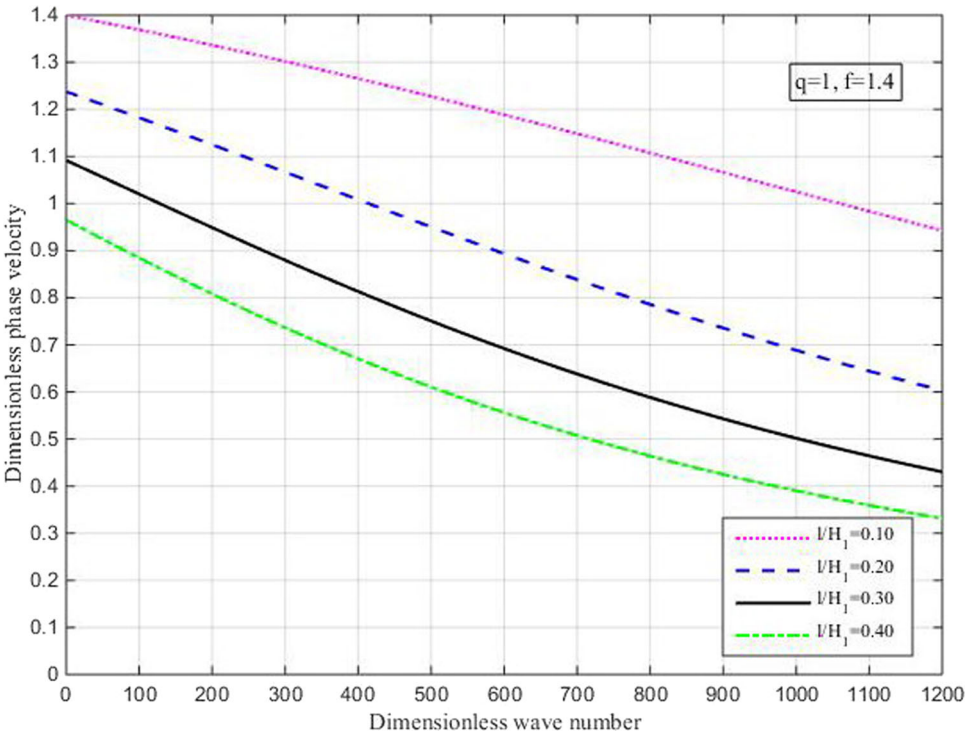


Fig. 17 Phase velocity (c/c_G) versus wave number (kH_2) for inhomogeneity parameter $q = 1$ and porosity factor $f = 1.4$

10 Conclusion

The propagation of Love waves in a transversely isotropic fluid-saturated porous layer with rigid boundary sandwiched between an isotropic homogenous layer and nonhomogeneous half space has been studied with parabolic irregularity at the interface of porous layer and half space. The dispersion equation for Love wave has been obtained and graphically plotted, showing the dimensionless phase velocity of Love waves versus the dimensionless wave number curves for different parameters. The numerical and graphical investigations have yielded the following significant key points:

Table 1 CPU time for each solution

Simulation	CPU hours	Simulation	CPU hours	Simulation	CPU hours	Simulation	CPU hours
Figure 2	0.1094	Figure 6	0.0313	Figure 10	0.1563	Figure 14	0.0781
Figure 3	0.1250	Figure 7	0.0625	Figure 11	0.1563	Figure 15	0.0938
Figure 4	0.1406	Figure 8	0.0938	Figure 12	0.5469	Figure 16	0.1406
Figure 5	0.0781	Figure 9	0.1406	Figure 13	0.1250	Figure 17	0.1094

1. The dispersion equation of the Love wave is a function of each layer's height (H_1 and H_2), irregularity's depth l, inhomogeneity parameter q, porosity f and wave number k. This implies that phase velocity of Love waves is dependent on these variables.
2. Figures 2, 3, 4, 5, 6, 7, 8 and 9 show that phase velocity diminishes with respect to wave number as the inhomogeneity parameter increases for each layer
3. Through Figs. 10, 11, 12 and 13, it is concluded that with the increment in anisotropy factor of the porous layer (M_2), the phase velocity decreases with the increase in wavenumber.
4. Through Figs. 14, 15, 16 and 17, it is observed that as the porosity of the porous layer (M_2) increases, the phase velocity decreases with the increase in wavenumber.
5. The phase velocity is decreasing as the size of the ratio of irregularity's depth to each layer's height is increasing indicating that the irregularity's size and shape have a significant effect on propagation of Love waves.

This research can be further extended by considering various parameters of the layer for example, the anisotropic porous layer could be modeled as a double porous layer, allowing for the exploration of the effects of two distinct types of pores. Another possible direction for extending this research involves examining different types of irregularities, such as triangular shapes. Additionally, multiple irregularities could be studied by considering multiple sources of disturbance in the half-space.

This study provides significant insights into the propagation of Love waves in an anisotropic porous situated between an isotropic layer and homogeneous half space with parabolic irregularity at the interface. However, several areas warrant further exploration. Future research could focus on extending the current model to account for more complex variables and boundary conditions. For instance, a double pours layer could be analyzed to explore the effect of two distinct types of pores can be explored (variable saturation levels in porous layers). Another possible direction for extending this research involves examining different types of irregularities, such as triangular shapes. Additionally, investigating multiple irregularities by considering multiple sources of disturbance in the half-space could provide better understanding of seismic behavior in natural environments. Experimental validation of the theoretical models would strengthen their practical applications in geophysics and earthquake engineering. Future research could also extend the current model by incorporating additional fluid properties such as viscosity and compressibility. Viscosity introduces internal friction within the fluid, causes energy dissipation, reducing wave amplitude. Additionally, compressibility affects how the fluid responds to pressure changes during wave passage, effecting medium's stiffness and phase velocity. Exploring these factors would provide deeper insights into the complex interactions between the fluid and solid matrix during seismic wave analysis.

11 Application of the model

The insights gained from this study on Love wave propagation through complex structures fluid-saturated porous layers inhomogeneous and irregular interfaces have significant real-world applications. This study offers valuable insights into seismic wave propagation in complex subsurface environments, advancing our understanding of ground response to seismic activity. It highlights the effects of porosity, anisotropy, and interface irregularities while contributing to the development of improved seismic imaging techniques. These insights play a critical role in more accurate earthquake risk assessments. In material science, the research examines how various materials and configurations influence seismic wave velocities, particularly in complex geological settings. In the oil and gas industry, the findings can also be applicable in the exploration and extraction processes. By investigating the propagation of surface waves through porous layers, the study aids in identifying reservoir characteristics and enhancing extraction techniques. It assists in mapping subsurface structures such as reservoirs, ultimately improving exploration and extraction processes. In civil engineering, the findings are relevant for designing infrastructure situated on or near non-homogeneous half-spaces. The soil-structure interaction is a key concern in such model, ensuring structures can endure dynamic loads from seismic forces. By examining factors like porosity, irregularities, and anisotropy in Earth models, this study enhances the precision of ground motion predictions. This ultimately improves earthquake hazard assessments and provides more resilient engineering practices.

Funding The authors declare that this research did not receive any specific grant from funding agencies in the public, commercial, or not-for-profit sectors. UGC-CSIR (998(CSIR-UGC NET DEC.2018)).

Data Availability Statement No data associated in the manuscript.

Declarations

Conflict of interest The authors declare that there are no conflict of interest regarding the publication of this paper. The authors confirm that they have no known competing financial interests or personal relationships that could have appeared to influence the work reported in this paper.

References

1. W. M.Ewing, W. S.Jardetzky, F.Press, Elastic waves in layered media. Geologiska Föreningen i Stockholm Förhandlingar **80**(1), 128–129 (1958)
2. D.Gubbins, *Seismology and plate tectonics* (Cambridge University Press, 1990)
3. M. A.Biot, Theory of propagation of elastic waves in a fluid-saturated porous solid. II. Higher frequency range. *The Journal of the acoustical Society of america*, *28*(2), 179–191 (1956)
4. M.A.Biot, Mechanics of deformation and acoustic propagation in porous media. J. Appl. Phys. **33**(4), 1482–1498 (1962)
5. H.Deresiewicz, The effect of boundaries on wave propagation in a liquid-filled porous solid: II. Love waves in a porous layer. *Bulletin of the Seismological Society of America*, *51*(1), 51–59. (1961)
6. A.Chattopadhyay, R. K. De, Love type waves in a porous layer with irregular interface. Int. J. Eng. Sci. **21**(11), 1295–1303 (1983)
7. N.C.Dutta, H.Odé, Attenuation and dispersion of compressional waves in fluid-filled porous rocks with partial gas saturation (White model)—Part I: Biot theory. Geophysics **44**(11), 1777–1788 (1979)
8. Y.S.Wang, Z.M.Zhang, Propagation of Love waves in a transversely isotropic fluid-saturated porous layered half-space. The Journal of the Acoustical Society of America **103**(2), 695–701 (1998)
9. S.Crampin, The basis for earthquake prediction. Geophys. J. Int. **91**(2), 331–347 (1987)
10. Z.Kon'czak, The propagation of Love waves in a fluid-saturated porous anisotropic layer. Acta Mech. **79**(3), 155–168 (1989)
11. J.M.Carcione, G.Seriani, Wave simulation in frozen porous media. J. Comput. Phys. **170**(2), 676–695 (2001)
12. M.D.Sharma, Surface waves in a general anisotropic poroelastic solid half-space. Geophys. J. Int. **159**(2), 703–710 (2004)
13. A.Chattopadhyay, P.Singh, P.Kumar, A.K.Singh, Study of Love-type wave propagation in an isotropic tri layers elastic medium overlying a semi-infinite elastic medium structure. Waves in Random and Complex Media **28**(4), 643–669 (2018)
14. L. L.Ke, Y.S.Wang, Z.M.Zhang, Propagation of Love waves in an inhomogeneous fluid saturated porous layered half-space with properties varying exponentially. J. Eng. Mech. **131**(12), 1322–1328 (2005)
15. L. L.Ke, Y. S.Wang, Z. M.Zhang, Love waves in an inhomogeneous fluid saturated porous layered half-space with linearly varying properties. Soil Dyn. Earthq. Eng. **26**(6–7), 574–581 (2006)
16. R.Kumar, D.K.Madan, & J. Singh Sikka, Shear wave propagation in multilayered medium including an irregular fluid saturated porous stratum with rigid boundary. *Advances in Mathematical Physics* (2014)
17. R.Kumar, D.K.Madan, J.S.Sikka, Wave propagation in an irregular fluid saturated porous anisotropic layer sandwiched between a homogeneous layer and half space. Wseas Transactions on Applied and Theoretical Mechanics **10**, 62–70 (2015)
18. R.Kakar, Dispersion of Love wave in an isotropic layer sandwiched between orthotropic and prestressed inhomogeneous half-spaces. Latin American Journal of Solids and Structures **12**, 1934–1949 (2015)
19. P.K.Vaishnav, S.Kundu , S.Gupta, and A.Saha, Propagation of Love-type wave in porous medium over an orthotropic semi-infinite medium with rectangular irregularity. *Mathematical Problems in Engineering* (2016)
20. S.Gupta, A.Chattopadhyay, D.K.Majhi, Effect of initial stress on propagation of Love waves in an anisotropic porous layer. Journal of Solid Mechanics **2**(1), 50–62 (2010)
21. S.Kundu, P.Alam, S.Gupta, D.K.Pandit, Impacts on the propagation of SH-waves in a heterogeneous viscoelastic layer sandwiched between an anisotropic porous layer and an initially stressed isotropic half space. J. Mech. **33**(1), 13–22 (2017)
22. R.Kumhar, S.Kundu, S.Gupta, Modelling of Love waves in fluid saturated porous viscoelastic medium resting over an exponentially graded inhomogeneous half-space influenced by gravity. Journal of Applied and Computational Mechanics **6**(3), 517–530 (2020)
23. R.Kumar, A.Goyal, A.Saini, Effect of Inhomogeneity and Triangular Irregularity on Propagation of Shear Waves in an Anisotropic Porous Layer. Mech. Solids **59**(2), 1036–1049 (2024)
24. R.Kumar, A.Saini, Influence of Parabolic Irregularity, Inhomogeneity, Initial Stress, and Anisotropy on Love Wave Propagation. Mech. Solids **59**(3), 1443–1458 (2024)
25. A.Saini, R.Kumar, Effect of Rigidity and Parabolic Irregularity on Love Wave Propagation in Transversely Isotropic Fluid-Saturated Porous Layer Lying over a Nonhomogenous Half-Space. Mech. Solids **59**(2), 1094–1107 (2024)
26. A.Saini, R.Kumar, Analysis of Love Waves in an Initially Stressed Transversely Isotropic Porous Layer Over Heterogeneous Half Space with Parabolic Irregularity. *Journal of Vibration Engineering & Technologies* p. 1–14, (2024)
27. A.Seikh, S.Shaw, B.Mukhopadhyay, Propagation of localized waves in a transversely isotropic thermoelastic layer of arbitrary thickness. The European Physical Journal Plus **138**(11), 1–15 (2023)
28. A.Chattopadhyay, S.Gupta, V.K.Sharma, P.Kumari, Stresses produced on a rough irregular half-space by a moving load. Acta Mech. **221**(3–4), 271–280 (2011)
29. M.A.Biot, Theory of elasticity and consolidation for a porous anisotropic solid. J. Appl. Phys. **26**(2), 182–185 (1955)
30. A.C.Eringen, J.C.Samuels, Impact and moving loads on a slightly curved elastic half-space (American Society of Mechanical Engineers, 1959)
31. H.F.Willis. Lv. a formula for expanding an integral as a series. The London, Edinburgh, and Dublin Philosophical Magazine and Journal of Science, 39(293):455–459. (1948)
32. C.J.Tranter, *Integral transform in mathematical physics, methuen & co* (Ltd, London, 1966), pp.63–67
33. H.Ding , W.Chen, and L. Zhang Elasticity of transversely isotropic materials, volume 126. Springer Science & Business Media. (2006)
34. A.E.H.Love, Mathematical Theory of Elasticity, Cambridge University Press, Cambridge (1920).

Springer Nature or its licensor (e.g. a society or other partner) holds exclusive rights to this article under a publishing agreement with the author(s) or other rightsholder(s); author self-archiving of the accepted manuscript version of this article is solely governed by the terms of such publishing agreement and applicable law.